

DARK MATTER ANNIHILATION AND DECAY PROFILES FOR THE RETICULUM II DWARF SPHEROIDAL GALAXY

VINCENT BONNIVARD¹, CÉLINE COMBET¹, DAVID MAURIN¹, ALEX GERINGER-SAMETH², SAVVAS M. KOUSHIAPPAS³,
MATTHEW G. WALKER², MARIO MATEO⁴, EDWARD W. OLSZEWSKI⁵, AND JOHN I. BAILEY III⁴*Draft version March 22, 2024*

ABSTRACT

The dwarf spheroidal galaxies (dSph) of the Milky Way are among the most attractive targets for indirect searches of dark matter. In this work, we reconstruct the dark matter annihilation (J -factor) and decay profiles for the newly discovered dSph Reticulum II. This is done using an optimized spherical Jeans analysis of kinematic data obtained from the Michigan/Magellan Fiber System (M2FS). We find Reticulum II to have one of the highest J -factor when compared to the other Milky Way dSphs. We have also checked the robustness of this result against several ingredients of the analysis. Unless it suffers from tidal disruption or significant inflation of its velocity dispersion from binary stars, Reticulum II may provide a unique window on dark matter particle properties.

Subject headings: galaxies: dwarf — galaxies: individual (Reticulum II) — dark matter — gamma rays: galaxies — methods: statistical — stars: kinematics and dynamics

1. INTRODUCTION

Along with the Galactic center and galaxy clusters, the dwarf spheroidal galaxies (dSph) of the Milky Way have been identified as promising targets for indirect dark matter (DM) searches (see recent reviews by Strigari 2013; Conrad et al. 2015). Their low astrophysical background, high mass-to-light ratio, and proximity make them compelling targets (Lake 1990; Evans et al. 2004). About twenty-five Galactic dSphs were known as of early 2015, and their observation by γ -ray telescopes has thus far shown no significant emission, leading to stringent constraints on $\langle\sigma_{\text{ann}}v\rangle$, the thermally-averaged DM self-annihilation cross-section (Acciari et al. 2010; Paiano et al. 2011; Abramowski et al. 2014; Geringer-Sameth et al. 2014; Fermi-LAT Collaboration 2015).

Recently, imaging data from the Dark Energy Survey has led to the discovery of nine new (potential) Milky-Way satellites in the Southern sky (Koposov et al. 2015; DES Collaboration et al. 2015). The nearest object, Reticulum II (Ret II, $d \sim 32$ kpc), is particularly intriguing, as evidence of γ -ray emission has been detected in its direction using the public Fermi-LAT data (Geringer-Sameth et al. 2015b; Hooper & Linden 2015). The Fermi-LAT collaboration simultaneously published a search for γ -ray emission from the newly discovered objects (Fermi-LAT Collaboration et al. 2015), based on the unreleased PASS8 dataset, and found no significant excess.

Nonetheless, and whatever the situation regarding a (non-)detection in this object might be, a robust determination of Ret II's DM content is crucial in or-

der to set constraints on the DM particle properties. Here, we reconstruct the DM annihilation and decay profiles of Ret II from a spherical Jeans analysis applied to stellar kinematic data obtained with the Michigan/Magellan Fiber System (M2FS) (Walker et al. 2015). We use the optimized Jeans analysis setup from Bonnivard et al. (2015a,b), described in Section 2. From the reconstructed DM density profiles, we then compute the astrophysical J - and D -factors, for annihilating and decaying DM respectively, and cross-check our results by varying different ingredients of the analysis (Section 3). Finally, we evaluate the ranking of Ret II among the most promising dSphs for DM indirect detection in Section 4.

2. ASTROPHYSICAL FACTORS, JEANS ANALYSIS AND DATA SETS

2.1. Astrophysical factors

The differential γ -ray flux coming from DM annihilation (resp. decay) in a dSph galaxy is proportional to the so-called ‘astrophysical’ factor J (resp. D) (Bergström et al. 1998),

$$J = \iint \rho_{\text{DM}}^2(l, \Omega) dl d\Omega \quad \left(\text{resp. } D = \iint \rho_{\text{DM}}(l, \Omega) dl d\Omega \right), \quad (1)$$

which corresponds to the integration along the line-of-sight (l.o.s.) of the DM density squared (resp. DM density) and over the solid angle $\Delta\Omega = 2\pi \times [1 - \cos(\alpha_{\text{int}})]$, where α_{int} is the integration angle. This quantity depends on both the extent of the DM halo and the mass density distribution, and is essential for putting constraints on the DM particle properties. All calculations of astrophysical factors are done with the CLUMPY code (Charbonnier et al. 2012), a new module of which has been specifically developed to perform the Jeans analysis⁶.

2.2. Jeans analysis

⁶ This upgrade will be publicly available in the soon-to-be released new version of the software (Bonnivard et al., in prep.).

bonnivard@lpsc.in2p3.fr
mgwalker@andrew.cmu.edu

¹ LPSC, Université Grenoble-Alpes, CNRS/IN2P3, 53 avenue des Martyrs, 38026 Grenoble, France

² McWilliams Center for Cosmology, Department of Physics, Carnegie Mellon University, Pittsburgh, PA 15213, USA

³ Department of Physics, Brown University, Providence, RI 02912, USA

⁴ University of Michigan, 311 West Hall, 1085 S. University Ave., Ann Arbor, MI 48109, USA

⁵ Steward Observatory, The University of Arizona, 933 N. Cherry Ave., Tucson, AZ 85721, USA

Several approaches have been developed to infer the DM density profile of dSph galaxies from stellar kinematic data (see recent reviews by Battaglia et al. 2013; Strigari 2013; Oswalt & Gilmore 2013). Here, we focus on the spherical Jeans analysis, which has been widely used for the determination of the astrophysical factors (Strigari et al. 2007; Essig et al. 2010; Charbonnier et al. 2011; Cholis & Salucci 2012; Geringer-Sameth et al. 2015a; Bonnavard et al. 2015b). We refer the reader to Bonnavard et al. (2015a) for a thorough description and motivation of the analysis setup we use in this work. Below, we briefly summarize the main ingredients.

Assuming steady-state, spherical symmetry, and negligible rotational support, the second-order Jeans equation can be obtained from the collisionless Boltzmann equation and reads (Binney & Tremaine 2008):

$$\frac{1}{\nu} \frac{d}{dr} (\nu \bar{v}_r^2) + 2 \frac{\beta_{\text{ani}}(r) \bar{v}_r^2}{r} = - \frac{GM(r)}{r^2}, \quad (2)$$

with $\nu(r)$ the stellar number density, $\bar{v}_r^2(r)$ the radial velocity dispersion, $\beta_{\text{ani}}(r) \equiv 1 - v_\theta^2/v_r^2$ the velocity anisotropy, and $M(r)$ the mass (assumed to be dominated by DM) enclosed within radius r . After solving Eq. (2) and projecting along the l.o.s. (as observations provide projected quantities only), the (squared) velocity dispersion at the projected radius R reads

$$\sigma_p^2(R) = \frac{2}{\Sigma(R)} \int_R^\infty \left(1 - \beta_{\text{ani}}(r) \frac{R^2}{r^2} \right) \frac{\nu(r) \bar{v}_r^2(r) r}{\sqrt{r^2 - R^2}} dr, \quad (3)$$

with $\Sigma(R)$ the surface brightness profile. We then compare the l.o.s. velocities of the stars to the projected velocity dispersion σ_p , computed using parametric forms for the unknown velocity anisotropy $\beta_{\text{ani}}(r)$ and DM density profile $\rho_{\text{DM}}(r)$. We do so using the following likelihood function (Strigari et al. 2007)

$$\mathcal{L} = \prod_{i=1}^{N_{\text{stars}}} \frac{(2\pi)^{-1/2}}{\sqrt{\sigma_p^2(R_i) + \Delta_{v_i}^2}} \exp \left[-\frac{1}{2} \left(\frac{(v_i - \bar{v})^2}{\sigma_p^2(R_i) + \Delta_{v_i}^2} \right) \right], \quad (4)$$

i.e. assuming a Gaussian distribution of l.o.s. stellar velocities v_i , centered on the mean stellar velocity \bar{v} , with a dispersion of velocities at the radius R_i coming from both the intrinsic dispersion $\sigma_p(R_i)$ and the measurement uncertainty Δ_{v_i} . Probability density functions (PDFs) of the anisotropy and DM parameters are obtained with a Markov Chain Monte Carlo (MCMC) engine⁷, and are used to compute the median and credible intervals (CIs) of the astrophysical factors for any integration angle.

Following the *optimized* Jeans analysis setup proposed in Bonnavard et al. (2015a), the DM density is described by an Einasto profile (e.g., Merritt et al. 2006), and the anisotropy and light profiles are given by Baes & van Hese (Baes & van Hese 2007) and Zhao-Hernquist (Hernquist 1990; Zhao 1996) parametrisations, respectively. The large freedom allowed by these parametrisations was found to mitigate some possible biases of the Jeans analysis (Bonnivard et al. 2015a). Finally, the extent of the DM halo is computed using the tidal radius estimation as in Bonnavard et al. (2015b).

⁷ We use the publicly available **GreAT** toolkit (Putze 2011; Putze & Derome 2014).

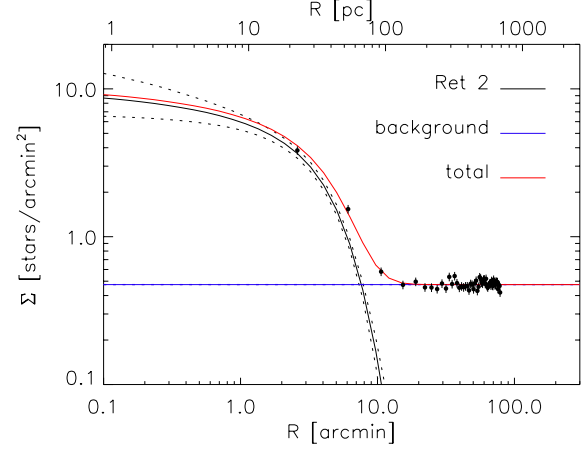


Figure 1. Projected stellar density profile of Ret II, derived from the photometric catalog of Koposov et al. (2015). Overplotted (red line) is the best-fitting model (we note that the fit is to the unbinned data), which is the sum of contributions from Ret II itself and a constant background (see Section 2.3). Dotted lines enclose 68% CIs for the projection of $\nu(r)$.

2.3. Data set

Surface brightness data— We fit the stellar number density profile $\nu(r)$ of Ret II following the procedure that Bonnavard et al. (2015b) use for ‘ultrafaint’ dwarfs (see their section 3.1). That is, we consider a flexible Zhao-Hernquist model for the 3D profile,

$$\nu^{\text{Zhao}}(r) = \frac{\nu_s^*}{(r/r_s^*)^\gamma [1 + (r/r_s^*)^\alpha]^{(\beta-\gamma)/\alpha}}, \quad (5)$$

where the five parameters are the normalization ν_s^* , the scale radius r_s^* , the inner power law index γ , the outer index β , and the transition parameter α . Along with an additional free parameter Σ_{bkd} that represents a uniform background density, these parameters then specify a model for the projected stellar density:

$$\Sigma_{\text{model}}(R) \equiv 2 \int_R^\infty \frac{\nu(r) r}{\sqrt{r^2 - R^2}} dr + \Sigma_{\text{bkd}}. \quad (6)$$

We fit this model to the photometric catalog generated by Koposov et al. (2015), which provides positions, colors and magnitudes of individual stars detected as point sources. From the raw catalog, we first identify possible members of Ret II as point sources (selected as sources with SExtractor ‘spread’ parameter < 0.01 in the g -band) whose extinction-corrected $g-r$ colors place them within 0.25 dex of the Dartmouth isochrone (Dotter et al. 2008), calculated for a stellar population with age 12 Gyr, metallicity $[\text{Fe}/\text{H}] = -2.5$, and distance modulus $m - M = 17.4$ (Koposov et al. 2015). To the unbinned distribution of projected positions for the $N = 12470$ RGB candidates identified within 1.5° of Ret II’s center, we fit 2D projections of $\nu(r)$ according to the likelihood function:

$$\mathcal{L}_2 \propto \prod_{i=1}^N \Sigma_{\text{model}}(R_i). \quad (7)$$

As in Bonnavard et al. (2015b), the fit is done with the software package MultiNest (Feroz & Hobson 2008; Feroz

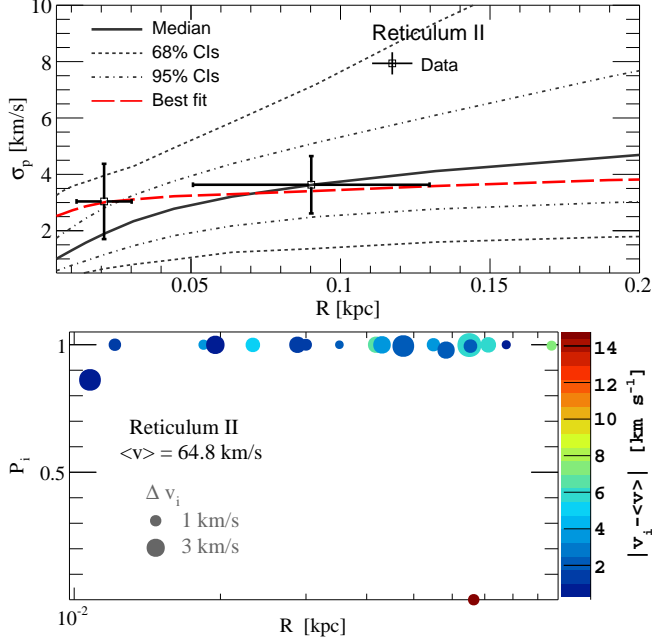


Figure 2. *Top:* velocity dispersion profile of Ret II and reconstructed median and credible intervals (solid and dashed black lines respectively), as well as best fit (long dashed red lines, shown for illustration purposes only). *Bottom:* distribution of membership probabilities as a function of the projected radius R and the departure from the mean velocity (z -axis, blue to red color) for the nineteen stars with $P_i \neq 0$. The size of the points is proportional to the velocity uncertainty. See text for discussion.

et al. 2009, 2013), and we use the samples from the posterior PDFs to propagate the light profile uncertainty in the Jeans analysis. Figure 1 shows the fit to the projected stellar density profile of Ret II (solid red line), with the contributions from Ret II itself and from the constant background (solid black and blue lines respectively).

Kinematic data— We use the Ret II stellar kinematic data set from Walker et al. (2015), obtained with M2FS. It consists of projected positions and l.o.s. velocities for 38 individual stars, as well as an estimation of their membership probability P_i . The latter, obtained using an expectation maximization algorithm (Walker et al. 2009), quantifies the probability that a given star belongs to the dSph or to the Milky Way foreground.

The top panel of Figure 2 presents the velocity dispersion profile of Ret II, as well as its reconstruction with the Jeans analysis⁸. The bottom panel of Figure 2 shows the distribution of membership probabilities as a function of the projected radius R and the departure from the mean velocity (color-coded from blue to red), for stars with non-zero P_i . As pointed out in Bonnavard et al. (2015b), a large fraction of stars with both intermediate P_i ($0.1 < P_i < 0.95$) and large departure from the mean velocity hints at Milky Way foreground contamination, which can affect the J - and D -factor reconstruction. For Ret II, only one star shows an intermediate P_i (Ret2-142 in the catalog of Walker et al. 2015, with $P_i = 0.86$), with a very small departure from the mean velocity estimated

Table 1

Astrophysical factors for Ret II ($d = 32$ kpc). For five different integration angles, the median J (resp D)-factors as well as their 68% and 95% CIs are given. Note that possible triaxiality of the dSph galaxies adds a systematic uncertainty of ± 0.4 (resp. ± 0.3) (Bonnivard et al. 2015a) and is not included in the quoted intervals.

α_{int} [deg]	$\log_{10}(J(\alpha_{\text{int}}))$ [$J/\text{GeV}^2 \text{ cm}^{-5}$] ^a	$\log_{10}(D(\alpha_{\text{int}}))$ [$D/\text{GeV cm}^{-2}$] ^b
0.01	$16.9^{+0.5(+1.1)}_{-0.4(-0.8)}$	$15.6^{+0.5(+1.0)}_{-0.3(-0.5)}$
0.05	$18.2^{+0.5(+1.0)}_{-0.4(-0.7)}$	$17.0^{+0.6(+1.0)}_{-0.3(-0.5)}$
0.1	$18.6^{+0.6(+1.1)}_{-0.4(-0.8)}$	$17.5^{+0.6(+1.1)}_{-0.4(-0.6)}$
0.5	$19.5^{+1.0(+1.6)}_{-0.6(-1.3)}$	$18.8^{+0.7(+1.2)}_{-0.7(-1.1)}$
1	$19.7^{+1.2(+2.0)}_{-0.9(-1.5)}$	$19.2^{+0.9(+1.4)}_{-0.9(-1.4)}$

^a $1 \text{ GeV}^2 \text{ cm}^{-5} = 2.25 \times 10^{-7} M_{\odot}^2 \text{ kpc}^{-5}$

^b $1 \text{ GeV cm}^{-2} = 8.55 \times 10^{-15} M_{\odot} \text{ kpc}^{-2}$

by Walker et al. (2015). Therefore we do not expect a strong sensitivity to foreground contamination. In this study, and as advocated in Bonnavard et al. (2015b), we use the data with $P_i > 0.95$ (seventeen likely members, one less than identified by Walker et al. 2015 after exclusion of Ret2-142) as our fiducial setup.

3. RESULTS

Figure 3 displays the J - (top) and D -factors (bottom) of Ret II, reconstructed from the Jeans/MCMC analysis, as a function of the integration angle α_{int} . Solid lines represent the median values, while dashed and dash-dot lines symbolize the 68% and 95% CIs respectively. Our data-driven Jeans analysis gives large statistical uncertainties due to the small size of the kinematic sample, and reflects our restricted knowledge of the DM content of this object. The CIs are comparable to those obtained for other ‘ultrafaint’ dSphs by Bonnavard et al. (2015b) (see also Figure 4). Table 1 summarizes our results for the astrophysical factors of Ret II.

We cross-checked our findings by varying different ingredients of the Jeans analysis. The resulting J -factors are shown in Figure 4. First, we ran the analysis using all 38 stars of the sample, but weighting the log-likelihood function of equation (4) by the membership probabilities P_i . Bonnavard et al. (2015b) find that a large difference between a P_i -weighted and a $P_i > 0.95$ analysis is another hint of contamination by Milky Way foreground stars. Here, the two analyses give very similar results, suggesting a clean sample for Ret II. We then randomly divide the kinematic sample in two parts, using one out of every two stars to build the two sub-samples. Applying the analysis to the two subsets leads to very similar J - and D -factors, which confirms that the reconstruction of the astrophysical factors is not significantly affected by outliers. We finally performed a binned Jeans analysis (see Charbonnier et al. 2011; Bonnavard et al. 2015b) of the kinematic data and found it to be compatible with our unbinned analysis.

⁸ The binned data and associated velocity dispersion reconstruction are only shown for illustration purposes. The final results are obtained with an analysis of unbinned data.

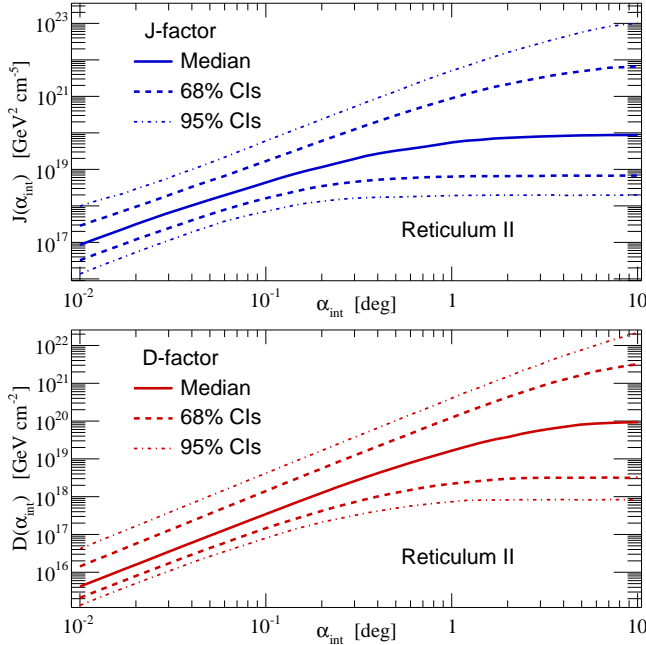


Figure 3. Median (solid), 68 % (dashed), and 95% (dash-dot) CIs of the J - (top) and D -factors (bottom) of Ret II, as a function of integration angle, reconstructed from our Jeans/MCMC analysis.

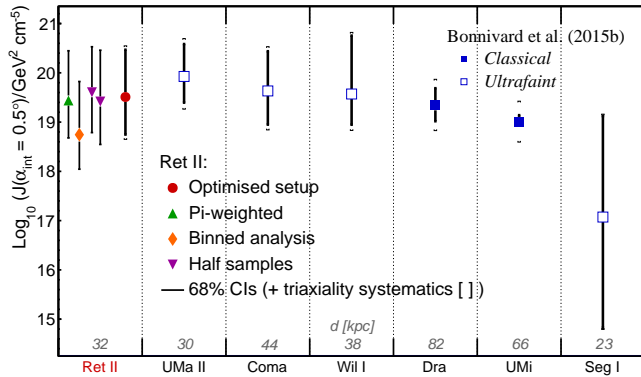


Figure 4. Comparison of the J -factors at $\alpha_{\text{int}} = 0.5^\circ$ obtained for Ret II (red circle) and for the potentially brightest objects from Bonnivard et al. (2015b) (blue squares), with the same Jeans/MCMC analysis. Ret II ranks as the second brightest dSph. A 0.4 dex systematic uncertainty was added in quadrature to the 68% CIs to account for possible triaxiality of the DM halo (Bonnivard et al. 2015a). Also shown are the J -factors obtained for Ret II by varying different ingredients of the analysis - see Section 3.

4. COMPARISON TO OTHER DSPHS

The same Jeans/MCMC analysis has been applied to twenty-one other dSphs in Bonnivard et al. (2015b). In Figure 4, we compare the J -factors (for $\alpha_{\text{int}} = 0.5^\circ$) of Ret II and of the brightest objects identified in Bonnivard et al. (2015b)⁹. Ret II is comparable to Wil I in terms of its median J -factor, but slightly below Coma and UMa II. Its CIs are typical of an ‘ultrafaint’ dSph, and significantly larger than the uncertainties of ‘classi-

cal’ dSphs.

Interpreting the possible γ -ray signal in Ret II in terms of DM annihilation (Geringer-Sameth et al. 2015b; Hooper & Linden 2015), one would expect similar emissions from the dSphs with comparable J -factors, such as UMa II, Coma, and Wil I. However, no excess was reported from these latter objects (Geringer-Sameth et al. 2014; Fermi-LAT Collaboration 2015). This could be explained by the large statistical and systematic¹⁰ uncertainties in the J -factors. Moreover, the Jeans analysis assumes all of these objects to be in dynamical equilibrium, but tidal interactions with the Milky Way could artificially inflate the velocity dispersion and therefore the astrophysical factors. UMa II, and to a lesser extent Coma, appear to be experiencing tidal disturbance (Simon & Geha 2007; Fellhauer et al. 2007; Muñoz et al. 2010; Smith et al. 2013), while Wil I may show non-equilibrium kinematics (Willman et al. 2011). Caution is therefore always advised when using/interpreting the astrophysical factors of these objects. The dynamical status of Ret II is not yet clear. Its flattened morphology may signal ongoing tidal disruption. However, the available kinematic data do not exhibit a significant velocity gradient that might be associated with tidal streaming motions (Walker et al. 2015).

5. CONCLUSION

We have applied a spherical Jeans analysis to the newly discovered dSph Ret II, using seventeen likely members from the kinematic data set of Walker et al. (2015). We employed the optimized setup of Bonnivard et al. (2015a,b), which was found to mitigate several biases of the analysis, and checked that our results are robust against several of its ingredients. We find that Ret II presents one of the largest annihilation J -factors among the Milky Way’s dSphs, possibly making it one of the best targets to constrain the DM particle properties. However, it is important to obtain follow-up photometric and spectroscopic data in order to test the assumptions of dynamical equilibrium as well as a negligible fraction of binary stars in the kinematic sample. Nevertheless, the proximity of Ret II and its potential large dark matter content make it the most interesting object from the newly discovered dwarf galaxies.

This work has been supported by the “Investissements d’avenir, Labex ENIGMASS”, and by the French ANR, Project DMAstro-LHC, ANR-12-BS05-0006. This study used the CC-IN2P3 computation center of Lyon. MGW is supported by National Science Foundation grants AST-1313045, AST-1412999. SMK is supported by DOE DE-SC0010010, NSF PHYS-1417505, and NASA NNX13AO94G. MM is supported by NSF grants AST-0808043 and AST-1312997. EWO is supported by NSF grant AST-0807498 and AST-1313006.

REFERENCES

Abramowski, A., Aharonian, F., Ait Benkhali, F., et al. 2014, Phys. Rev. D, 90, 112012

⁹ Segue I, often considered as one of the best targets, may have a highly uncertain J -factor (Bonnivard, Maurin & Walker, in prep.). We show it only for illustration purposes.

¹⁰ The latter comes from a possible triaxiality of the dSph (0.4 and 0.3 dex for annihilation and decay respectively, see Bonnivard et al. 2015a), and depends on the l.o.s. orientation with respect to the principle axes of the halo.

- Acciari, V. A., Arlen, T., Aune, T., & et al. 2010, *ApJ*, 720, 1174
- Baes, M., & van Hese, E. 2007, *A&A*, 471, 419
- Battaglia, G., Helmi, A., & Breddels, M. 2013, *New Astronomy Review*, 57, 52
- Bergström, L., Ullio, P., & Buckley, J. H. 1998, *Astroparticle Physics*, 9, 137
- Binney, J., & Tremaine, S. 2008, *Galactic Dynamics: Second Edition* (Princeton University Press)
- Bonnivard, V., Combet, C., Maurin, D., & Walker, M. G. 2015a, *MNRAS*, 446, 3002
- Bonnivard, V., Combet, C., Daniel, M., et al. 2015b, *ArXiv e-prints*, arXiv:1504.02048
- Charbonnier, A., Combet, C., & Maurin, D. 2012, *Computer Physics Communications*, 183, 656
- Charbonnier, A., Combet, C., Daniel, M., et al. 2011, *MNRAS*, 418, 1526
- Cholis, I., & Salucci, P. 2012, *Phys. Rev. D*, 86, 023528
- Conrad, J., Cohen-Tanugi, J., & Strigari, L. E. 2015, *ArXiv e-prints*, arXiv:1503.06348
- DES Collaboration, Bechtol, K., Drlica-Wagner, A., et al. 2015, *ArXiv e-prints*, arXiv:1503.02584
- Dotter, A., Chaboyer, B., Jevremović, D., et al. 2008, *ApJS*, 178, 89
- Essig, R., Sehgal, N., Strigari, L. E., Geha, M., & Simon, J. D. 2010, *Phys. Rev. D*, 82, 123503
- Evans, N. W., Ferrer, F., & Sarkar, S. 2004, *Phys. Rev. D*, 69, 123501
- Fellhauer, M., Evans, N. W., Belokurov, V., et al. 2007, *MNRAS*, 375, 1171
- Fermi-LAT Collaboration. 2015, *ArXiv e-prints*, arXiv:1503.02641
- Fermi-LAT Collaboration, The DES Collaboration, Drlica-Wagner, A., et al. 2015, *ArXiv e-prints*, arXiv:1503.02632
- Feroz, F., & Hobson, M. P. 2008, *MNRAS*, 384, 449
- Feroz, F., Hobson, M. P., & Bridges, M. 2009, *MNRAS*, 398, 1601
- Feroz, F., Hobson, M. P., Cameron, E., & Pettitt, A. N. 2013, *ArXiv e-prints*, arXiv:1306.2144
- Geringer-Sameth, A., Koushiappas, S. M., & Walker, M. 2015a, *ApJ*, 801, 74
- Geringer-Sameth, A., Koushiappas, S. M., & Walker, M. G. 2014, *ArXiv e-prints*, arXiv:1410.2242
- Geringer-Sameth, A., Walker, M. G., Koushiappas, S. M., et al. 2015b, *ArXiv e-prints*, arXiv:1503.02320
- Hernquist, L. 1990, *ApJ*, 356, 359
- Hooper, D., & Linden, T. 2015, *ArXiv e-prints*, arXiv:1503.06209
- Koposov, S. E., Belokurov, V., Torrealba, G., & Wyn Evans, N. 2015, *ArXiv e-prints*, arXiv:1503.02079
- Lake, G. 1990, *Nature*, 346, 39
- Merritt, D., Graham, A. W., Moore, B., Diemand, J., & Terzić, B. 2006, *AJ*, 132, 2685
- Muñoz, R. R., Geha, M., & Willman, B. 2010, *AJ*, 140, 138
- Oswalt, T. D., & Gilmore, G., eds. 2013, *Dark Matter in the Galactic Dwarf Spheroidal Satellites* (Springer Reference), 1039
- Paiano, S., Lombardi, S., Doro, M., et al. 2011, *ArXiv:1110.6775*, arXiv:1110.6775
- Putze, A. 2011, *International Cosmic Ray Conference*, 6, 260
- Putze, A., & Derome, L. 2014, *Phys.Dark Univ.*, doi:10.1016/j.dark.2014.07.002
- Simon, J. D., & Geha, M. 2007, *ApJ*, 670, 313
- Smith, R., Fellhauer, M., Candlish, G. N., et al. 2013, *MNRAS*, 433, 2529
- Strigari, L. E. 2013, *Phys. Rep.*, 531, 1
- Strigari, L. E., Koushiappas, S. M., Bullock, J. S., & Kaplinghat, M. 2007, *Phys. Rev. D*, 75, 083526
- Walker, M. G., Mateo, M., Olszewski, E. W., et al. 2015, submitted
- Walker, M. G., Mateo, M., Olszewski, E. W., Sen, B., & Woodroffe, M. 2009, *AJ*, 137, 3109
- Willman, B., Geha, M., Strader, J., et al. 2011, *AJ*, 142, 128
- Zhao, H. 1996, *MNRAS*, 278, 488